NIH Public Access
Author Manuscript
Mol Cell. Author manuscript; available in PMC 2010 December 11.

Published in final edited form as:
Mol Cell. 2009 December 11; 36(5): 819–830. doi:10.1016/j.molcel.2009.11.028.

The pseudo-active site of ILK is essential for its binding to α-parvin and localization to focal adhesions

Koichi Fukuda[1], **Sudhiranjan Gupta**[1], **Ka Chen**[2], **Chuanyue Wu**[2], and **Jun Qin**[1,*]

[1]Department of Molecular Cardiology, Lerner Research Institute, Cleveland Clinic Foundation, 9500 Euclid Avenue, Cleveland, OH 44195, USA

[2]Department of Pathology, University of Pittsburgh School of Medicine, 3550 Terrace Street, Pittsburgh, PA 15261, USA

Summary

Integrin-linked kinase (ILK) plays a pivotal role in connecting transmembrane receptor integrin to the actin cytoskeleton and thereby regulating diverse cell adhesion-dependent processes. The kinase domain (KD) of ILK is indispensable for its function, but the underlying molecular basis remains enigmatic. Here we present the crystal structure of the ILK KD bound to its cytoskeletal regulator, the C-terminal calponin homology domain of α-parvin. While maintaining a canonical kinase fold, the ILK KD displays a striking pseudo-active site conformation. We show that rather than performing the kinase function, this conformation specifically recognizes α-parvin for promoting effective assembly of ILK into focal adhesions. The α-parvin-bound ILK KD can simultaneously engage integrin β cytoplasmic tails. These results thus define ILK as a distinct pseudokinase that mechanically couples integrin and α-parvin for mediating cell adhesion. They also highlight functional diversity of the kinase fold and its "active" site in mediating many biological processes.

Introduction

The communication between transmembrane integrin receptors and the actin cytoskeleton is fundamental for cell migration, spreading and differentiation. Integrin-linked kinase (ILK) is one of the few essential and evolutionarily conserved mediators in this communication process (Wu, 2004;Legate et al., 2006). Originally identified as an integrin β cytoplasmic tail (CT) binding protein, ILK was thought to be composed of an N-terminal ankyrin repeat domain, a middle pleckstrin homology (PH)-like motif, and a C-terminal kinase domain (KD) (Hannigan et al., 1996). Cell biological and biochemical data have continued to mount, establishing ILK as a key molecule in coupling integrins with the actin cytoskeleton (for review, see Legate et al., 2006). The importance of such ILK-dependent coupling has been underscored by several elegant genetic analyses in *Drosophila* (Zarvas et al., 2001), *Caenorhabditis elegans*

* To whom correspondence should be addressed: Jun Qin, Department of Molecular Cardiology, Mail Code NB20, Lerner Research Institute, Cleveland Clinic Foundation, 9500 Euclid Avenue, Cleveland, OH 44195, USA, +1 (216)-444-5392 (Phone); +1 (216)-445-1466 (Fax) qinj@ccf.org.

Accession Numbers

The atomic coordinates have been deposited in the Protein Data Bank (accession codes: 3KMU and 3KMW).

Supplemental Data

Supplementary Data that include experimental procedures, 7 figures, their legends, and references can be found with this article online at http://www.molecule.org/supplemental/.

Publisher's Disclaimer: This is a PDF file of an unedited manuscript that has been accepted for publication. As a service to our customers we are providing this early version of the manuscript. The manuscript will undergo copyediting, typesetting, and review of the resulting proof before it is published in its final citable form. Please note that during the production process errors may be discovered which could affect the content, and all legal disclaimers that apply to the journal pertain.

NIH-PA Author Manuscript
NIH-PA Author Manuscript
NIH-PA Author Manuscript

NIH-PA Author Manuscript

NIH-PA Author Manuscript

NIH-PA Author Manuscript

(Mackinnon et al., 2002), and mice (Sakai et al., 2003), which showed that depletion or dysregulation of ILK leads to severe defects in the integrin-containing cytoskeleton structure and cell adhesion dynamics. Despite the overwhelming information about the biological importance of ILK, the precise molecular underpinning of ILK function remains elusive. In particular, while ILK has been widely claimed to act as a signaling serine-threonine kinase to trigger diverse integrin signaling pathways (Hannigan et al., 2005), its catalytic function has been under significant debate (Hannigan et al., 2005;Legate et al., 2006) since genetic analyses indicated that ILK kinase activity may not be required for normal tissue development and function (Zarvas et al., 2001;Mackinnon et al., 2002;Sakai et al., 2003;Dai et al., 2006;Kanasaki et al., 2008). Examination of the ILK KD primary sequence suggested a pseudokinase function of the protein with some variations in the putative catalytic site (Boudeau et al., 2006;Scheeff et al., 2009), but many cell-based analyses reported that ILK was capable of directly phosphorylating diverse substrates including a generic substrate myelin basic protein (MBP) and physiological targets (for review, see Hannigan et al., 2005) such as integrin β1 CT (Hannigan et al., 1996), myosin light chain kinase (Deng et al., 2001), β-parvin (Yamaji et al., 2001), and Akt/PKB (Persad et al., 2001). The ILK kinase activity was also shown to be significantly enhanced by several co-factors including PIP3 (Delcommenne et al., 1998), the C-terminal calponin homology domain (CH2) of α-parvin (Attwell et al., 2003), and the actin monomer sequestering protein, thymosin β4 (Bock-Marquette et al., 2004;Fan et al., 2009).

Although variations in the primary sequences of the catalytic motifs are often used to predict whether a protein has catalytic function or not, recent 3D structural analyses indicated that this sequence-based approach is not always valid. For example, WNK kinase, which lacks the conserved catalytic lysine residue in the subdomain II (replaced by C250) that corresponds to K72 in protein kinase PKA), was found to use K233 in its β2 strand as an alternative catalytic lysine (Min et al., 2004). Also, CASK, which was initially thought to be catalytically inactive due to the lack of the DFG aspartate that can coordinate a functional magnesium ion (Mg), was shown to be catalytically active in an Mg-independent manner (Mukherjee et al., 2008). Given the highly conflicting data yet central importance of ILK in biology, a definitive structure-function analysis on ILK KD is necessary to define the precise mechanism of ILK function. To this end, we have determined the crystal structure of the ILK KD bound to its putative activator α-parvin CH2. Our structure revealed a distinct pseudo-active site in ILK thus defining it as a pseudokinase. More detailed analysis demonstrated that ILK lacks intrinsic kinase activity, yet utilizes its pseudo-active site to recognize α-parvin for focal adhesion targeting. While pseudokinases are emerging as an important class of protein regulators (Boudeau et al., 2006), exactly how they function remains largely unknown. Our results provide significant insight into this class of proteins. In particular, the pseudo-active site-mediated target binding not only helps to elucidate the mechanism of ILK but also sheds light upon the functional diversity of the kinase fold and its “active” site in mediating diverse cellular events.

Results

Structure Determination

A series of constructs comprising the C-terminal KD of ILK was examined for expression but produced highly insoluble ILK aggregates, precluding further structural analysis. Based on the previous reports that α-parvin CH2 (therein CH2) binds to ILK KD (Tu et al., 2001) and activates it (Attwell et al., 2003), we constructed a bicistronic coexpression system (Tan, 2001) to co-express CH2 with a human ILK fragment (183-452) containing the putative PH domain and KD (Hannigan et al., 1996). This approach yielded a soluble and mono-dispersed complex suitable for the structural analysis. We crystallized and solved the structure of the complex at 1.8 Å resolution. We also co-crystallized the complex in the presence of ATP and Mg and solved the structure at 2.0 Å resolution (Table 1). The structures are well defined except

NIH-PA Author Manuscript

NIH-PA Author Manuscript

NIH-PA Author Manuscript

for the short N-terminal region in CH2, which exhibits poor density maps with relatively higher temperature factors (B-factors) compared to the overall values. This region is known to bind to another partner paxillin LD1 motif (Wang et al., 2008; Lorenz et al., 2008).

ILK KD contains a canonical kinase fold but an unusual ATP-Mg binding mode

The overall fold of ILK KD is very similar to those of known kinases and contains characteristic bilobal domains (Knighton et al., 1991), namely, the N-terminal lobe that folds into a five-stranded anti-parallel β-sheet flanked by a short and a long (αC) α-helix, and the C-terminal lobe that contains a bundle of α-helices and a short pair of anti-parallel β-strands (β7-β8) (Figs. 1A and S1A). ATP is situated in a nucleotide-binding cleft between the two lobes (Figs. 1A and S1A) similar to the ATP binding site in other kinases (Manning et al., 2002) (Figs. S1B and S1C). Superposition of the ILK KD structure (ATP-bound form) onto the nucleotide-bound active conformation of PKA, a representative serine-threonine kinase (PDB entry 1ATP) reveals a similar global architecture with an RMSD of 2.4 Å (21% identity) (Fig. S1D). The well-defined ATP molecule in the ILK structure was surprising since previous sequence-based analysis suggested that ILK may not bind ATP due to a dramatically altered ATP binding loop (P-loop) where the well-conserved glycine-rich GXGXXG motif (X denotes any residue) in Ser-Thr kinases is replaced by a non-glycine-rich NENHSG motif in ILK (Scheeff et al., 2009). It was equally surprising that ATP was not hydrolyzed in the ILK structure since even inactive kinases such as MEK1 hydrolyze ATP into ADP (Fischmann et al., 2009) - the first step in the kinase reaction. However, despite the similar binding site, ATP in ILK has an unusual binding mode as compared to known kinases such as PKA: (i) ATP coordinates only one Mg in ILK whereas two Mgs are bound to ATP in PKA to facilitate catalysis (Fig. 1B). (ii) The tri-phosphate orientations of ATP, especially the β-γ phosphate groups in ILK are drastically different from those in PKA (Fig. 1C). Notably, the side chain of K341 from the activation loop of ILK (corresponding to glycine in the well-known DFG motif, see Fig. S1E) protrudes against the ATP phosphate groups and coordinates the γ-phosphate of ATP (Fig. 1B). Such distinct coordination might facilitate the distinct γ phosphate orientation as compared to that in PKA (Fig. 1B). Also, K220 in ILK bridges α- and γ-phosphates of ATP, whereas the equivalent lysine residue in known kinases (K72 in PKA) coordinates α and β-phosphates of ATP (Figs. 1D and S1F). (iii) ATP bound to the P-loop of ILK, is far away from the putative catalytic loop (Figs. 1D and 1E) whereas in known kinases, ATP, especially the γ-phosphate, is very close to the catalytic loop for catalysis (Figs. 1D and 1E). The Gly-rich P-loop is conformationally flexible to allow the bound ATP to interact with the catalytic loop (e.g., PKA in Fig. 1E). By contrast, the non-glycine-rich P-loop in ILK appears to lack such flexibility as indicated by low temperature factors, and thus no movement was observed with and without ATP (Fig. 1E). This lack of flexibility explains why the bound ATP in ILK remains distant from the catalytic loop (Fig. 1E).

ILK KD has a severely degraded catalytic core

The structure-based sequence alignment of ILK with representative kinases reveals that the catalytic loop in ILK diverges severely with significant insertion/deletion and absence of multiple catalytically important residues (Fig. S1E). In particular, our structure shows that the invariant catalytic base aspartate (D166 in PKA) in the hallmark HRD motif is replaced by a neutral residue A319 in ILK KD (Fig. 1E). This aspartate in PKA is known to properly orient the γ-phosphate and to accept a substrate hydroxyl moiety for phospho-transfer (Madhusudan et al., 1994;Zheng et al., 1993) (Fig. 1B). However, the corresponding residue A319 in ILK KD is not only hydrophobic but far away (~9-10Å) from the γ-phosphate of ATP (largely due to the inflexibility of the ATP-bound P-loop, see Fig. 1E) as compared to PKA (Figs. 1B and 1E). Inspection of the structure revealed no structurally alternative Asp or any similar and conserved residues near the catalytic loop (Fig. 1D). The significance of the conserved Asp is underscored by a recent study of the pseudokinase STRADα, in which the corresponding Asp

NIH-PA Author Manuscript

NIH-PA Author Manuscript

NIH-PA Author Manuscript

is replaced by a serine (Baas et al., 2003). Other notable changes of the catalytic loop in ILK include N321, which corresponds to the catalytic lysine K168 in PKA that is involved in phospho-transfer, and S324, which corresponds to the catalytic aspargine N171 in PKA that coordinates the second Mg (Fig. 1E) and forms hydrogen-bond with the backbone carbonyl of D166. Here, although S324 hydroxyl group makes similar hydrogen bond with the backbone carbonyl of corresponding A319 in ILK, it does not coordinate with Mg since the second Mg is absent. Together with the above finding that the ATP γ-phosphate is geometrically far away from the catalytic loop (Fig. 1E), the deviations in the catalytic core indicate that ILK cannot perform the catalysis as a conventional kinase. The unusual structural arrangement also provides a strong clue as to why ATP was not hydrolyzed by ILK.

ILK has a distinct putative activation loop

The activation loop of protein kinase is known to dynamically regulate kinase activity, especially substrate entry into the catalytic core. The activation loop of ILK spans from the DVK motif (residue 339-341 that corresponds to the DFG motif in known kinases) to the APE motif (residues 357-359 that corresponds to the C-terminal end of the P+1 loop) (Nolen et al., 2004) (Fig. S1E). Strikingly, the activation loop in ILK is significantly short and also lacks a highly conserved phosphorylation site known to regulate the conformation of the activation loop in conventional kinases (e.g., T197 in PKA) (Figs. 2A and S1E). The activation loops in typical kinases are disordered and become ordered upon phosphorylation, thus transitioning a kinase from an inactive to an active state (Nolen et al., 2004). Conversely, the activation loop in the ILK structure is well ordered without any phosphorylation (Figs. 1A and 2A). Notably, the mean B-values of the ILK activation loop are relatively low at 19.3 $Å^2$ compared to 21.7 $Å^2$ for the whole ILK KD, indicating that this segment is quite rigid. This is likely due to the extensive hydrophobic and hydrophilic interactions between the activation loop and the N-lobe containing the αC helix (Fig. 2B). In particular, the side chain hydroxyl oxygen of S343 makes a hydrogen bond with the side chain of E238 in the αC-helix, and the two phenylalanine residues (F342 and F344) in the activation loop that sandwich S343 pack tightly against a cluster of hydrophobic residues, L222, V224, W227, and L267 in the N-lobe core and F235 and L242 in the αC-helix (Fig. 2B). Note that S343 was proposed to be a phosphorylation site for ILK activation (Persad et al., 2001) but our structure shows that S343 hydroxyl group is buried in the activation loop/N-lobe interface (Fig. 2B) and important for the structural integrity. Thus, the side chain of S343 is not freely accessible for phosphorylation contrasting to that observed in T197 in PKA for inducing the kinase activation. No direct experimental evidence has been reported for the S343 phosphorylation. Furthermore, a phosphorylation-mimic S343D mutation caused no effect on the ILK activation (see below).

The substitution of the canonical DFG in functional kinases with DVK in ILK also makes the activation loop distinct. The side chain conformation of D339 in the DVK motif of ILK is markedly different from those in the DFG motifs of typical kinases such that D339 only coordinates to one metal whereas the aspartate in DFG coordinates two metal ions (Fig. 1B) to promote the catalysis. Two residues are inserted immediately preceding D339 (Fig. S1E), which may lead to the distinct side chain orientation of D339 and unusual metal coordination involving this residue. More strikingly, ILK lacks the DFG glycine that allows the DFG to flip in (active) or out (inactive) during kinase activation (Fig. S2). As a result, the DVK motif of ILK appears to be locked in a “flipped in” position with or without ATP (Fig. S2), a structural feature consistent with the rigidity of ILK activation loop.

ILK KD is different from atypical kinases

Structures of several atypical Ser/Thr kinases have been reported including Titin (Mayans et al., 1998), WNK (Min et al., 2004), and CASK (Mukherjee et al., 2008). Titin and WNK have remarkable ways to compensate for missing catalytic residues by alternative residues/motifs,

NIH-PA Author Manuscript

NIH-PA Author Manuscript

NIH-PA Author Manuscript

i.e., the EFG glutamate in Titin acts as the DFG aspartate in typical kinases (Mayans et al., 1998) and the K233 residue in the β2 strand of WNK acts as the catalytic lysine equivalent to K72 in PKA (Min et al., 2004). CASK lacks two conserved Mg binding residues (corresponding to N171 and D184 in PKA) (Fig. S1E) and thus it functions as an Mg-independent kinase that selectively phosphorylates neurotoxin (Mukherjee et al., 2008). Importantly, these three kinases are atyptical because of an altered Mg binding site, but all retain the glycine-rich P-loop, the well-conserved catalytic loop, and very similar activation segment (Fig. S1E), which seem to be sufficient for kinase activity. By contrast, these hallmark features are significantly disrupted in ILK, i.e., the unusual ATP binding configuration, severely impaired catalytic core, and a short and rigid activation loop. No spatially conserved residues/motifs in the ILK structure were found to possibly compensate for these non-permissive catalytic features (Fig. 1D).

Functional analysis shows that ILK lacks kinase activity

Although ILK has been widely regarded as a key serine-threonine kinase in integrin signaling (for reviews, see Hannigan et al., 2005; Legate et al., 2006), the above structural findings strongly suggested that ILK may be a pseudokinase, which prompted us to critically re-evaluate the ILK catalytic activity. The previously claimed ILK kinase activity was largely based on the cell-based assays or partially purified ILK. We thus decided to first perform kinase assays using purified recombinant ILK. As mentioned above, ILK alone is not soluble, so we co-expressed full-length ILK with PINCH LIM1-2 that binds to the N-terminal ankyrin repeat domain of ILK but does not affect the target binding and putative catalytic activity of the ILK KD (Chiswell et al., 2008; Yang et al., 2009). Using the PINCH-LIM1-2-ILK complex purified from bacteria, we observed no kinase activity on previously reported substrates including myelin basic protein (MBP, generic kinase substrate) (Hannigan et al., 1996; Kim et al., 2009), integrin β CT (Hannigan et al., 1996), and CH2 (Yamaji et al., 2001) (Fig. 3A). Recombinant ILK from commercial source (Randox Life Sciences, Inc) had no kinase activity either (data not shown). In comparison, bacteria-purified PKA and MEK kinases phosphorylated MBP very potently (Fig. 3A). We next asked if ILK can be activated via mutation or co-factors. Previous cell-based studies showed that ILK may be activated by phosphorylation-mimic S343D mutation (Persad et al., 2001) or co-factors including PIP3 (Delcommenne et al., 1998) and α-parvin CH2 (Attwell et al., 2003). However, purified ILK exhibited no activity upon S343D mutation or other potentially activating mutations or addition of the above co-factors (Fig. 3B). In fact, PIP3 did not even bind to ILK (data not shown) and the previously suggested PH motif is an integral part of the P-loop in our structure (Figs. S3A-S3C). Varying Mg concentrations in the kinase assays also had no effect. We next sought to perform kinase assays using endogenous ILK purified directly from chick-tissue (Deng et al., 2001). Although the chick tissue-purified proteins containing ILK phosphorylated generic MBP as previously demonstrated (Deng et al., 2001) (Fig. 3C), it had no effect on previously suggested physiological substrates of ILK including integrin β CT (data not shown) and Akt (Fig. 4). Furthermore, the MBP phosphorylation was not enhanced at all by CH2 that was reported to be an ILK activator (Attwell et al., 2003) (Fig. 3C). In fact, as we show below, CH2 binds tightly to the putative substrate site (the P+1 loop and G-helix), and thus its addition to the kinase reaction would inhibit the phosphorylation of MBP if the effect were directly mediated by ILK. However, no inhibitory effect was observed (Fig. 3C).

The most widely studied ILK target is Akt (for review, see Hannigan et al., 2005), and ILK-mediated Akt activation was shown to be enhanced by the actin-monomer sequestering protein thymosin β4 (Bock-Marquette et al., 2004; Fan et al., 2009). We thus performed kinase assays to specifically examine this effect. As shown in Fig. 4A, purified recombinant ILK and ILK S343D mutant showed no effect on Akt phosphorylation in the absence and presence of thymosin β4. Endogenous ILK purified from chick tissue also showed no effect on Akt in the

NIH-PA Author Manuscript

NIH-PA Author Manuscript

NIH-PA Author Manuscript

absence and presence of thymosin β4 (Fig. 4B). In fact, in pull-down assays, we failed to see any direct interaction between thymosin β4 and ILK (data not shown), suggesting that the thymosin β4 effect on Akt (Bock-Marquette et al., 2004; Fan et al., 2009) might be indirect. Finally, we attempted to repeat the previously reported effect of ILK on Akt using co-immunoprecitated ILK (Persad et al., 2001). However, ILK co-precipitated from HEK 293 cells expressing FLAG-full-length ILK also had no effect on the Akt phosphorylation (Figs. 4C and 4D). It remains to be determined what factors caused the discrepancy between our assay and previous assays (Persad et al., 2001). It is possible that co-precipitation assays might involve an unknown kinase associated with ILK. Consistently, a large >500 kDa supramolecular complex containing ILK was reported to phosphorylate Akt, but some unknown components in this complex, not the co-precipitated ILK, was found to be responsible for the effect (Hill et al., 2002). Interestingly, we found that ILK is always co-purified with α-parvin and PINCH as a tight ternary complex from the tissue extracts (Fig. S4), supporting an emerging theme that ILK forms a functional heterotrimer in cells to mediate cytoskeleton assembly and cell adhesion (Wu, 2004; Legate et al., 2006).

A distinct binding interface between ILK KD and α-parvin CH2

Given the above structural and functional data that indicated ILK KD is catalytically inactive and may act as an adaptor, a key question is then how exactly ILK KD exerts its adapting function *via* its kinase fold. It was also puzzling to us why α-parvin or α-parvin CH2 had no effect on ILK activity (Figs. 3 and 4) given the previously identified role of CH2 as an ILK activator (Attwell et al., 2003). We thus examined the structure of the ILK KD-CH2 complex in detail, which revealed strikingly that CH2 recognizes a protruding surface in the C-lobe of the ILK KD that comprises a pair of α-helices (αEF-helix; αG-helix) and a small part of the C-terminal activation loop (P+1) in the ILK KD (Fig. 5A). The interface is quite large with the buried surface area of ~1,900 A^2 that is a typical range for the high affinity complex (Lo Conte et al., 1999) (Figs. 5B and S5A-S5C). The corresponding αG-helix and the C-terminal activation loop in ILK are parts of the active site in known kinases, which are involved in substrate or regulator binding (Song et al., 2001;Kim et al., 2005;Dar et al., 2005). Such binding mode is similar to conventional kinase-target interaction as exemplified by PKR-eIF2α (kinase-substrate) and PKA-RIα (kinase-regulator) (Figs. S5D-S5G). However, the ILK-α-parvin interaction is highly specific since the residues in ILK that contact CH2 are not conserved in other kinases (Fig. S1E). In particular, the M402-K403 residues in the ILK G-helix that make the most extensive contact with CH2 (Fig. 5C) are not conserved in other kinases. To further elucidate the importance of this specific interaction, we designed a double mutation (M402A/K403A) of ILK KD. Figure 5D shows that the double mutation completely disrupted the parvin binding to ILK *in vivo* and dramatically impaired the localization of ILK to sites of FAs (Figs. 5E-5H). These data strongly demonstrate that the ILK-parvin interaction is important for the ILK localization to FAs. As a comparison, the ATP binding defective mutations did not affect the ILK localization to FAs (Figs. S5H-S5K).

The ILK binding interface on CH2 is also distinct from that for paxillin that binds the N-terminal region of CH2 (Wang et al., 2008; Lorenz et al., 2008). Overall, we have uncovered a distinct binding mode to α-parvin mediated by the pseudo-kinase active site of ILK. Importantly, the CH2 binding site in ILK also structurally rules out the possibility of α-parvin as an ILK kinase activator (Attwell et al., 2003) and explains the functional data (Figs. 3 and 4). Furthermore, our data provide a structural basis as to how ILK KD acts as a unique adaptor to engage α-parvin for FA assembly.

The α-parvin-bound ILK KD can physically link to integrin cytoplasmic face

Since ILK KD was suggested to bind to integrin β CT to link integrin to focal adhesions and cytoskeleton (Hannigan et al., 1996), we asked whether the ILK KD in its tight complex with

NIH-PA Author Manuscript

NIH-PA Author Manuscript

NIH-PA Author Manuscript

the CH2 can still bind the integrin β CTs. Remarkably, our GST-pull down assays showed that the CH2-bound ILK KD can effectively interact with both integrin β1 and β3 CTs (Figs. 6A and 6B), and α-parvin did not prevent the integrin binding to ILK (Figs. 6C and 6D). The full-length ILK in the absence of CH2 could also bind to both the integrin β1 and β3 CTs, as expected (Figs. 6E and 6F). These data indicate that the binding sites for integrin and parvin on the ILK KD do not physically overlap. Since the integrin β1 CT binding site was previously mapped to within the residues (293-451) of ILK KD (Hannigan et al., 1996), we examined the surface features of this fragment in our structure, which revealed that integrin may bind to a conserved distal hydrophobic surface of the ILK kinase C-lobe (Fig. S6). Although the precise binding site remains to be experimentally evaluated, this model explains how ILK KD acts as a distinct platform for multi-protein assembly, promoting the dynamic regulation of integrin-mediated FA assembly and the integrin-cytoskeleton linkage.

Discussion

In this study, we have obtained high resolution structure of ILK KD-α-parvin CH2 complex, which provides the first definitive insight into a pseudokinase function of ILK incapable of performing the catalysis. Extensive kinase assays using both recombinant and endogenous ILK with and without putative activators (Figs. 3 and 4) strongly support our structure-based conclusion, but contradict with previous cell biological and biochemical data. The disagreement may arise from different experimental conditions. In particular, partially pure ILK samples used in the previous studies might have caused kinase activity *via* unknown kinases associated with ILK. Consistent with this possibility, we found that while partially purified ILK from the chick tissue phosphorylated MBP (Fig. 3), which was also shown before (Deng et al., 2001) (Fig. 3), it did not phosphorylate the putative physiological substrates such as integrin and Akt (Figs. 3 and 4). Furthermore, the phosphorylation effect was not affected at all by the addition of excess α-parvin, which would strongly inhibit the phosphorylation based on our structure (Fig. 3). Thus, great care must be taken when interpreting the results of catalytic functions derived from the partially pure samples or indirect cellular effect. Note that although we have tested the previously reported ILK substrates, it is theoretically impossible to exclude the possibility of a yet-unidentified unusual substrate for ILK, but such possibility seems unlikely because ILK does not even hydrolyze ATP - the first step of kinase reaction against any substrate.

In addition to ILK KD, three other pseudokinases (VRK3, ROP2, and STRADα) have been structurally characterized (Scheeff et al., 2009; Labesse et al., 2009; Zeqiraj et al., 2009). VRK3 and ROP2 do not bind ATP due to a substantially altered P-loop (one Gly is replaced by Met), and thus it is straightforward to classify them as pseudokinases. STRADα has several major missing catalytic features, including an altered P-loop, degenerated catalytic loop, altered DFG motif, and altered Mg binding site. These abnormal structural features are reminiscent to those in ILK. Intriguingly, the γ-phosphate of the bound ATP in STRADα is also disconnected from the degraded catalytic loop as similarly found in ILK (Figs. S7A-S7C). Such disconnection would preclude the formation of the transition state during phosphoryl-transfer even if the catalytic base was not degenerated (Cheng et al., 2005). Indeed, despite having an active conformation, STRADα was found to be catalytically inactive and also ATP was bound without hydrolysis (Zeqiraj et al., 2009). By contrast, the pseudo-active sites of STRADα and ILK have significant differences such as a shortened activation loop in ILK vs. STRADα. The two proteins are involved in completely different biological processes. A phylogenetic tree analysis indicated that STRADα and ILK may have evolved from two distinct kinase subfamilies: STRADα from STLK (Set-like kinase) whereas ILK from MLK (mixed-lineage kinase) (Manning et al., 2002).

NIH-PA Author Manuscript

NIH-PA Author Manuscript

NIH-PA Author Manuscript

Because of the dramatically altered catalytic motifs and the significantly short activation loop in ILK, it is less straightforward to determine precisely whether the overall structure of ILK KD mimics an active or inactive conformation of a kinase. Interestingly, using a recently developed Local Spatial Pattern protocol (Kornev et al., 2008) for examining the active or inactive conformations of kinases, we found that the overall structure of ILK KD seems to adopt a putative active conformation since it has two well-defined hydrophobic C- and R-spine motifs characteristic of active protein kinase conformations (Fig. 7). α-parvin does not seem to significantly affect this conformation since its binding site in ILK involves the conserved helices (αEF and αG) and part of P+1 loop, which are not drastically different between inactive and active kinases. Other structurally characterized pseudokinases also adopt active conformations including VRK3 and ROP2 (Scheeff et al., 2009; Labesse et al., 2009) and STRADα (in the presence of ATP and regulator MO25) (Zeqiraj et al., 2009). Preservation of active conformations of pseudokinases may be a general feature for their functions. In the case of ILK, the pseudo-active site conformation is involved in specifically recognizing α-parvin. The striking similarity of such recognition mode to the known kinase-substrate interaction (Fig. S5) suggests an interesting evolutionary consequence that pseudokinases may all use their pseudo-active sites for protein-protein interactions. The specificity of these pseudo-active site-mediated interactions may be determined by the conformations and sequences of the individual pseudo-active sites. Indeed, the G-helix orientation in ILK deviates somewhat from those of other kinase-substrate or kinase-inhibitor structures (Fig. S5G) and such deviation may be critical for the spatial specificity of ILK KD to recognize parvin. The specificity is crucial for the targeting of ILK to FAs (Fig. 5). Upon its targeting to FAs, ILK KD may further bind to other molecules such as integrin (Figs. 6 and S6) and kindlins (Tu et al., 2003) to trigger supramolecular FA assembly. What then regulates the ILK-α-parvin dissociation? ATP does not seem to play a significant role since the ILK-α-parvin complex interface is essentially identical with and without ATP. Interestingly, phosphorylation of α-parvin was shown to reduce its binding to ILK (Yang et al., 2005), suggesting that the phosphorylation may induce a conformational change of α-parvin to inhibit the CH2 binding to ILK. Although the exact mechanism remains to be determined, the α-parvin phosphorylation may provide one pathway for regulating the disassembly of ILK-mediated supramolecular complex during FA turnover.

In summary, the detailed structural and functional analysis now allows us to firmly establish ILK as a distinct pseudokinase. Our results not only resolve a longstanding controversy about the ILK kinase activity but also provide significant structural insight into how ILK regulates the integrin-cytoskeleton linkage *via* the integrin-ILK-parvin pathway. The conserved kinase fold but distinct pseudo-substrate active site in binding to α-parvin indicates that ILK might have evolved from an ancestral protein common to a protein kinase family but diverged during evolution to become a distinct scaffold protein. Given a crucial role of pseudokinase domain from nearly 10% of the human kinome in regulating the assembly of signaling complexes (Manning et al., 2002), our finding also paves the way for further elucidating the function of pseudokinase as a distinct protein-protein interaction module.

Experimental Procedures

Cloning and Plasmid Construction

The bicistronic coexpression vector of the ILK KD-α-parvin CH2 complex was created by the standard subcloning strategy. Briefly, the genes encoding the human α-parvin CH2 domain (residues 248-372) (Wang et al., 2008) and the human ILK KD (residues 183-452) were amplified by PCR, and subcloned into the first and second translation cassettes of the polycistronic coexpression vector pST39 (Tan, 2001), respectively. The two variant surface cysteine residues of ILK across species were engineered to serine residues (C346S; C422S) to increase the protein solubility of the ILK KD-α-parvin CH2 complex, whereas wild type ILK

NIH-PA Author Manuscript

NIH-PA Author Manuscript

NIH-PA Author Manuscript

(full length and KD) was used for the functional assays. A hexahistidine tag preceding a thrombin cleavage sequence was incorporated at immediately preceding the CH2 sequence. The coexpression plasmid of the ILK KD-α-parvin (full-length) complex was also created using the same strategy. The gene encoding the full-length human α-parvin was subcloned into the pET15b vector (Novagen). For coexpression of full-length ILK bound to PINCH LIM1-2, the genes encoding the human PINCH LIM1-2 (residues 1-127) and the full-length ILK (residues 1-452) were subcloned into the pST39 vector, as the above. A maltose-binding protein (MBP) gene was incorporated at the immediately preceding the PINCH LIM1-2 gene to generate the MBP-fused PINCH LIM1-2. Site-directed mutagenesis was carried out by QuikChange Site-Directed Mutagenesis Kit (Stratagene) using appropriate primer sets. All constructs were verified by the DNA sequencing analysis.

Protein Expression and Purification

All recombinant proteins were expressed in *Escherichia coli*, and their purifications were performed using affinity chromatography followed by further conventional chromatography steps. Detailed procedures are described in the supplementary information.

Crystallization

The crystals of the ILK KD-CH2 complex (apo form) were grown at 4°C by hanging drop vapor diffusion method by mixing equal volumes of the protein solution (~0.2 mM) and a reservoir solution consisting of 0.05 M Bis-Tris Propane, pH 6.8, 12% (w/v) polyethylene glycol 5,000 mono methyl ether, 5% (v/v) 1-propyl alcohol. The co-crystals of the MgATP bound form were also grown in the similar condition as above.

Data Collection, Structure Determination, and Refinement

Details of the data collection, structure determination and refinement are provided in the supplementary information.

In Vitro Radioactive Kinase Assay

The kinase assay was performed using the standard protocol from Upstate Biotechnology (see details in the supplementary information). The kinase assay was also performed by another previously reported protocol (Persad et al., 2001) and the results of these two protocols were found to be the same.

DNA Transfection, Immunoprecipitation, and Immunofluorescence Staining

Human HeLa cells were transfected with DNA vectors encoding GFP or GFP-tagged wild type ILK or ILK mutants using Lipofectamine Plus (Invitrogen). The details of immunoprecipitation and focal adhesion localization assays are provided in supplementary information.

In Vitro Integrin Binding Assay

The binding experiments of integrin β1 CT and β3 CT to the ILK proteins (full-length or KD) were performed using the GST-pull down assays (see details in the supplementary information).

Supplementary Material

Refer to Web version on PubMed Central for supplementary material.

NIH-PA Author Manuscript

NIH-PA Author Manuscript

NIH-PA Author Manuscript

Acknowledgments

We are grateful to Dr. Peter Zwart and the staff at Lawrence Berkeley National Laboratory, and Drs. Zingwei Huang and Yongjun Zhang for technical assistance. We thank Drs. Song Tan for providing polycistronic coexpression vectors, Edward Plow, Shoukat Dedhar and other members of the Qin laboratory for useful discussions. This work was supported by grants from the NIH (J.Q. and C.W.) and AHA (S.G).

References

Attwell S, Mills J, Troussard A, Wu C, Dedhar S. Integration of cell attachment, cytoskeletal localization, and signaling by integrin-linked kinase (ILK), CH-ILKBP, and the tumor suppressor PTEN. Mol Biol Cell 2003;14:4813–4825. [PubMed: 12960424]

Baas AF, Boudeau J, Sapkota GP, Smit L, Medema R, Morrice NA, Alessi DR, Clevers HC. Activation of the tumor suppressor kinase LKB1 by the STE20-like pseudokinase STRAD. EMBO J 2003;22:3062–3072. [PubMed: 12805220]

Bock-Marquette I, Saxena A, White MD, Dimaio JM, Srivastava D. Thymosin β4 activates integrin-linked kinase and promotes cardiac cell migration, survival, and cardiac repair. Nature 2004;432:466–472. [PubMed: 15565145]

Boudeau J, Miranda-Saavedra D, Barton GJ, Alessi DR. Emerging roles of pseudokinases. Trends Cell Biol 2006;16:443–452. [PubMed: 16879967]

Cheng Y, Zhang Y, McCammon JA. How does the cAMP-dependent protein kinase catalyze the phosphorylation reaction: an *ab initio* QM/MM atudy. J Am Chem Soc 2005;127:1553–1562. [PubMed: 15686389]

Chiswell BP, Zhang R, Murphy JW, Boggon TJ, Calderwood DA. The structural basis of the integrin-linked kinase-PINCH interactions. Proc Natl Acad Sci USA 2008;105:20677–20682. [PubMed: 19074270]

Dai C, Stolz DB, Bastacky SI, St-Arnaud R, Wu C, Dedhar S, Liu Y. Essential role of integrin-linked kinase in podocyte biology: Bridging the integrin and slit diaphragm signaling. J Am Soc Nephrol 2006;17:2164–2175. [PubMed: 16837631]

Dar AC, Dever TE, Sicheri F. Higher-order substrate recognition of eIF2α by the RNA-dependent protein kinase PKR. Cell 2005;122:887–900. [PubMed: 16179258]

Delcommenne M, Tan C, Gray V, Rue L, Woodgett J, Dedhar S. Phosphoinositide-3-OH kinase-dependent regulation of glycogen synthase kinase 3 and protein kinase B/Akt by the integrin-linked kinase. Proc Natl Acad Sci USA 1998;95:11211–11216. [PubMed: 9736715]

Deng JT, Van Lierop JE, Sutherland C, Walsh MP. Ca^{2+}-independent smooth muscle contraction. A novel function for integrin-linked kinase. J Biol Chem 2001;276:16365–16373. [PubMed: 11278951]

Fan Y, Gong Y, Ghosh PK, Graham LM, Fox PL. Spatial coordination of actin polymerization and ILK-Akt2 activity during endothelial cell migration. Dev Cell 2009;16:661–674. [PubMed: 19460343]

Fischmann TO, Smith CK, Mayhood TW, Myers JE, Reichert P, Mannarino A, Carr D, Zhu H, Wong J, Yang RS, et al. Crystal structures of MEK1 binary and ternary complexes with nucleotides and inhibitors. Biochemistry 2009;48:2661–2674. [PubMed: 19161339]

Hannigan GE, Leung-Hagesteijn C, Fitz-Gibbon L, Coppolino MG, Radeva G, Filmus J, Bell JC, Dedhar S. Regulation of cell adhesion and anchorage-dependent growth by a new β1-integrin-linked protein kinase. Nature 1996;379:91–96. [PubMed: 8538749]

Hannigan G, Troussard AA, Dedhar S. Integrin-linked kinase: a cancer therapeutic target unique among its ILK. Nature Rev Cancer 2005;5:51–63. [PubMed: 15630415]

Hill MM, Feng J, Hemmings BA. Identification of a plasma membrane raft-associated PKB Ser473 kinase activity that is distinct from ILK and PDK1. Curr Biol 2002;12:1251–1255. [PubMed: 12176337]

Kanasaki K, Kanda Y, Palmsten K, Tanjore H, Lee SB, Lebleu VS, Gattone VH Jr, Kalluri R. Integrin β1-mediated matrix assembly and signaling are critical for the normal development and function of the kidney glomerulus. Dev Biol 2008;313:584–593. [PubMed: 18082680]

Kim C, Xuong NH, Taylor SS. Crystal structure of a complex between the catalytic and regulatory (RIα) subunits of PKA. Science 2005;307:690–696. [PubMed: 15692043]

NIH-PA Author Manuscript

NIH-PA Author Manuscript

NIH-PA Author Manuscript

Kim M, Ogawa M, Fujita Y, Yoshikawa Y, Nagai T, Koyama T, Nagai S, Lange A, Fässler R, Sasakawa C. Bacteria hijack integrin-linked kinase to stabilize focal adhesions and block cell attachment. Nature 2009;459:578–582. [PubMed: 19489119]

Knighton DR, Zheng JH, Ten Eyck LF, Ashford VA, Xuong NH, Taylor SS, Sowadski JM. Crystal structure of the catalytic subunit of cyclic adenosine monophosphate-dependent protein kinase. Science 1991;253:407–414. [PubMed: 1862342]

Kornev AP, Taylor SS, Ten Eyck LF. A helix scaffold for the assembly of active protein kinases. Proc Natl Acad Sci USA 2008;105:14377–14382. [PubMed: 18787129]

Labesse G, Gelin M, Bessin Y, Lebrun M, Papoin J, Cerdan R, Arold ST, Dubrematz JF. ROP2 from *Toxoplasma gondii*: a virulence factor with a protein-kinase fold and no enzymatic activity. Structure 2009;17:139–146. [PubMed: 19141290]

Legate KR, Montanez E, Kudlacek O, Fässler R. ILK, PINCH and parvin: the tIPP of integrin signalling. Nature Rev Mol Cell Biol 2006;7:20–31. [PubMed: 16493410]

Lo Conte L, Chothia C, Janin J. The atomic structure of protein-protein recognition sites. J Mol Biol 1999;285:2177–2198. [PubMed: 9925793]

Lorenz S, Vakonakis I, Lowe ED, Campbell ID, Noble ME, Hoellerer MK. Structural analysis of the interactions between paxillin LD motifs and α-parvin. Structure 2008;16:1521–1531. [PubMed: 18940607]

Mackinnon AC, Qadota H, Norman KR, Moerman DG, Williams BD. *C. elegans* PAT-4/ILK functions as an adaptor protein within integrin adhesion complexes. Curr Biol 2002;12:787–797. [PubMed: 12015115]

Madhusudan, Trafny EA, Xuong NH, Adams JA, Ten Eyck LF, Taylor SS, Sowadski JM. cAMP-dependent protein kinase: crystallographic insights into substrate recognition and phosphotransfer. Protein Sci 1994;3:176–187. [PubMed: 8003955]

Manning G, Whyte DB, Martinez R, Hunter T, Sudarsanam S. The protein kinase complement of the human genome. Science 2002;298:1912–1934. [PubMed: 12471243]

Mayans O, van der Ven PF, Wilm M, Mues A, Young P, Fürst DO, Wilmanns M, Gautel M. Structural basis for activation of the titin kinase domain during myofibrillogenesis. Nature 1998;395:863–869. [PubMed: 9804419]

Min X, Lee BH, Cobb MH, Goldsmith EJ. Crystal structure of the kinase domain of WNK1, a kinase that causes a hereditary form of hypertension. Structure 2004;12:1303–1311. [PubMed: 15242606]

Mukherjee K, Sharma M, Urlaub H, Bourenkov GP, Jahn R, Sudhof TC, Wahl MC. CASK functions as a Mg^{2+}-independent neurexin kinase. Cell 2008;133:328–339. [PubMed: 18423203]

Nolen B, Taylor S, Ghosh G. Regulation of protein kinases: controlling activity through activation segment conformation. Mol Cell 2004;15:661–675. [PubMed: 15350212]

Persad S, Attwell S, Gray V, Mawji N, Deng JT, Leung D, Yan J, Sanghera J, Walsh MP, Dedhar S. Regulation of protein kinase B/Akt-serine 473 phosphorylation by integrin-linked kinase: critical roles for kinase activity and amino acids arginine 211 and serine 343. J Biol Chem 2001;276:27462–27469. [PubMed: 11313365]

Sakai T, Li S, Docheva D, Grashoff C, Sakai K, Kostka G, Braun A, Pfeifer A, Yurcheno PD, Fässler R. Integrin-linked kinase (ILK) is required for polarizing the epiblast, cell adhesion, and controlling actin accumulation. Genes Dev 2003;17:926–940. [PubMed: 12670870]

Scheeff ED, Eswaran J, Bunkoczi G, Knapp S, Manning G. Structure of the pseudokinase VRK3 reveals a degraded catalytic site, a highly conserved kinase fold, and a putative regulatory binding site. Structure 2009;17:128–138. [PubMed: 19141289]

Song H, Hanlon N, Brown NR, Noble MEM, Johnson LN, Barford D. Phosphoprotein interactions revealed by the crystal structure of kinase-associated phosphatase in complex with phosphoCDK2. Mol Cell 2001;7:615–626. [PubMed: 11463386]

Tan S. A modular polycistronic expression system for overexpressing protein complexes in *Escherichia coli*. Protein Exp Purif 2001;21:224–234.

Tu Y, Huang Y, Zhang Y, Hua Y, Wu C. A new focal adhesion protein that interacts with integrin-linked kinase and regulates cell adhesion and spreading. J Cell Biol 2001;153:585–598. [PubMed: 11331308]

NIH-PA Author Manuscript

NIH-PA Author Manuscript

NIH-PA Author Manuscript

Tu Y, Wu S, Shi X, Chen K, Wu C. Migfilin and Mig-2 link focal adhesions to filamin and the actin cytoskeleton and function in cell shape modulation. Cell 2003;113:37–47. [PubMed: 12679033]

Wang X, Fukuda K, Byeon IJ, Velyvis A, Wu C, Gronenborn A, Qin J. The structure of α-parvin CH2-paxillin LD1 complex reveals a novel modular recognition for focal adhesion assembly. J Biol Chem 2008;283:21113–21119. [PubMed: 18508764]

Wu C. The PINCH-ILK-parvin complexes: assembly, functions and regulation. Biochim Biophys Acta 2004;1692:55–62. [PubMed: 15246679]

Yamaji S, Suzuki A, Sugiyama Y, Koide Y, Yoshida M, Kanamori H, Mohri H, Ohno S, Ishigatsubo Y. A novel integrin-linked kinase-binding protein, affixin, is involved in the early stage of cell-substrate interaction. J Cell Biol 2001;153:1251–1264. [PubMed: 11402068]

Yang Y, Guo L, Blattner SM, Mundel P, Kretzler M, Wu C. Formation and phosphorylation of the PINCH-1-integrin linked kinase-α-parvin complex are important for regulation of renal glomerular podocyte adhesion, architecture, and survival. J Am Soc Nephrol 2005;16:1966–1976. [PubMed: 15872073]

Yang Y, Wang X, Hawkins CA, Chen K, Vaynberg J, Mao X, Tu Y, Zuo X, Wang J, Wang YX, et al. Structural basis of focal adhesion localization of LIM-only adaptor PINCH by integrin-linked kinase. J Biol Chem 2009;284:5836–5844. [PubMed: 19117955]

Zarvas CG, Gregory SL, Brown NH. Drosophila integrin-linked kinase is required at sites of integrin adhesion to link the cytoskeleton to the plasma membrane. J Cell Biol 2001;152:1007–1018. [PubMed: 11238456]

Zeqiraj E, Filippi BM, Goldie S, Navratilova I, Boudeau J, Deak M, Alessi DR, van Aalten DM. ATP and MO25α regulate the conformational state of the STRADα pseudokinase and activation of the LKB1 tumour suppressor. PLoS Biol 2009;7:e1000126. [PubMed: 19513107]

Zheng J, Knighton DR, Ten Eyck LF, Karlsson R, Xuong N, Taylor SS, Sowadski JM. Crystal structure of the catalytic subunit of cAMP-dependent protein kinase complexed with MgATP and peptide inhibitor. Biochemistry 1993;32:2154–2161. [PubMed: 8443157]

NIH-PA Author Manuscript
NIH-PA Author Manuscript
NIH-PA Author Manuscript

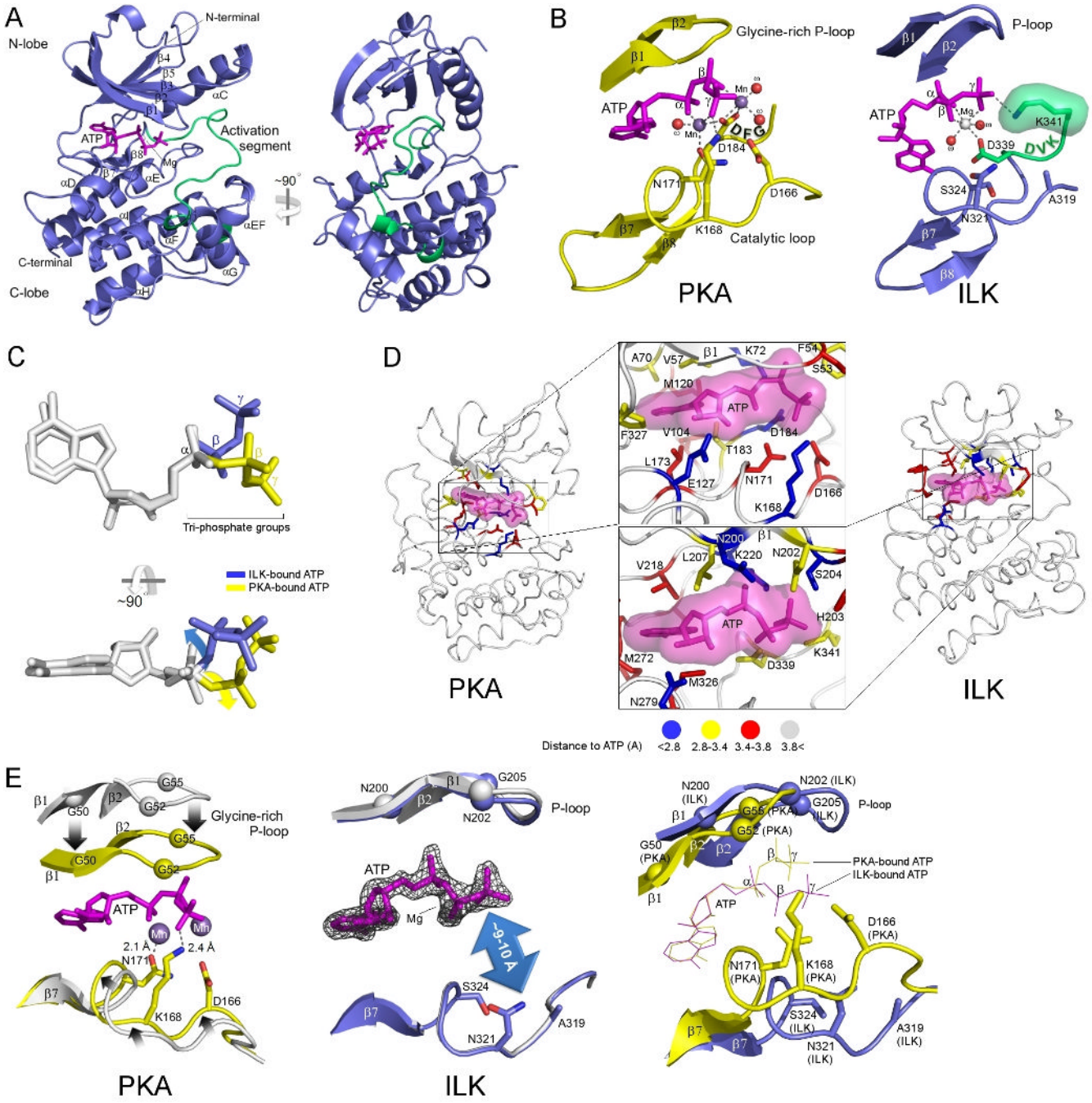

Figure 1. Structure of ILK KD and its Comparison with PKA

(**A**) Ribbon drawing of the ILK KD structure (blue) in the presence of MgATP. ATP and the activation segment are colored in magenta and green, respectively. The CH2 structure is removed from the panel for simplicity. (**B**) Structural comparison of the ATP-binding pocket between ILK and PKA. Left: Close-up view of the active site of PKA (PDB entry 1ATP) in the presence of ATP (magenta) and two Mn atoms (purple sphere). D166, K168, and N171 in the catalytic loop and the DFG aspartate (D184) are depicted in stick models. Right: Close-up view of the ATP-binding site in the ILK structure. Residues that are structurally equivalent to those in PKA are depicted in stick models. The DVK motif in the activation segment is highlighted in green, and the K341 residue is depicted in stick and surface models. (**C**)

NIH-PA Author Manuscript

NIH-PA Author Manuscript

NIH-PA Author Manuscript

Comparison of the ATP conformations bound to ILK and PKA. The adenine-ring and ribose are superposed, and the β-γ phosphate groups bound in ILK and PKA are colored in blue and yellow, respectively. (**D**) Comparison of the ATP-binding sites between ILK and PKA. Left: The overall structure of the ATP-bound PKA. The residues that contact ATP within 3.8 Å are colored. The ATP molecule is shown in stick model (magenta) with transparent surface. Center top: Close-up view of the ATP-binding residues in PKA. Center bottom: Close-up view of the ATP-binding residues in ILK. Right: The overall structure of the ATP-bound ILK. (**E**) Comparison of the ATP-binding P-loop dynamics. Left: The glycine-rich P-loop movement in PKA upon ATP binding. The structures of ATP-bound PKA and its apo form (PDB entry 1J3H) are colored in yellow and white, respectively. The selected C_α atoms in the P-loop are rendered in spheres. Center: The P-loop conformation of the ILK KD. The coordinates of the ILK KD in the MgATP-bound (blue) and free (white) are superimposed, and the selected triplet residues that are structurally equivalent to those in the PKA catalytic loop are depicted. The ATP molecule is superimposed with the 2.0-Å F_o-F_c omit electron density map contoured at 4σ level. Right: Comparison of the P-loop and the catalytic loop of PKA with their equivalent regions of ILK. The PKA-bound ATP (yellow) is overlaid at the adenine-ring and ribose groups onto the ILK-bound ATP (blue) by a rigid-body superposition. See also Figure S1.

NIH-PA Author Manuscript
NIH-PA Author Manuscript
NIH-PA Author Manuscript

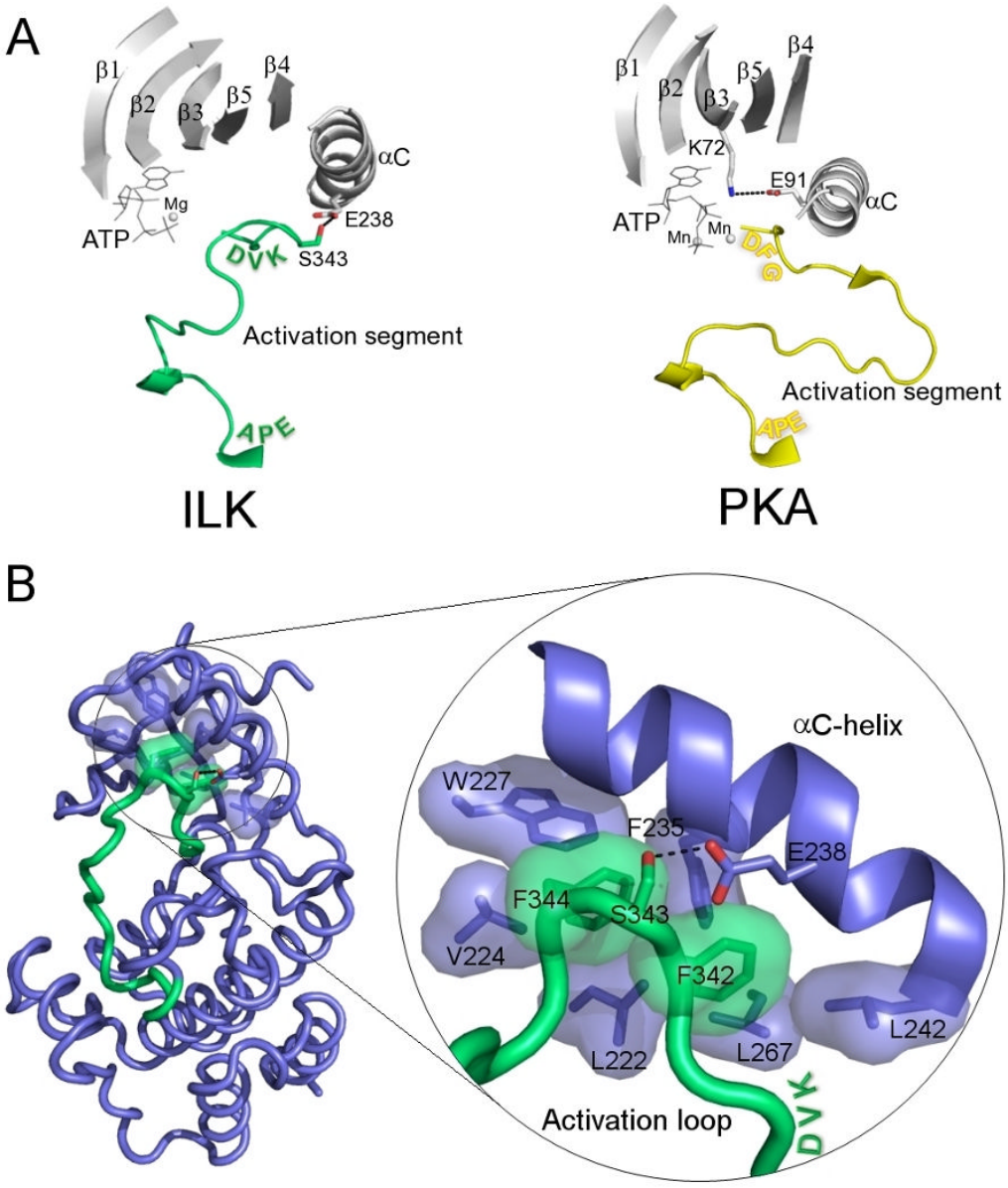

Figure 2. Structural Comparison of the Activation Segment

(**A**) An orthogonal view of the activation segment. Left: The activation segment (green) in ILK KD. The side chains of S343 and E238 (αC-helix) are depicted in stick models. Right: The activation segment (yellow) in PKA. (**B**) Divergent activation segment in the ILK KD structure. Left: Overall tube model of the ILK KD and the location of the activation segment that can interact with a cluster of hydrophobic residues in the N-lobe. Right: A detailed view of hydrophobic and polar interactions formed between the activation segment and the N-lobe (<4 Å). See also Figure S2.

NIH-PA Author Manuscript

NIH-PA Author Manuscript

NIH-PA Author Manuscript

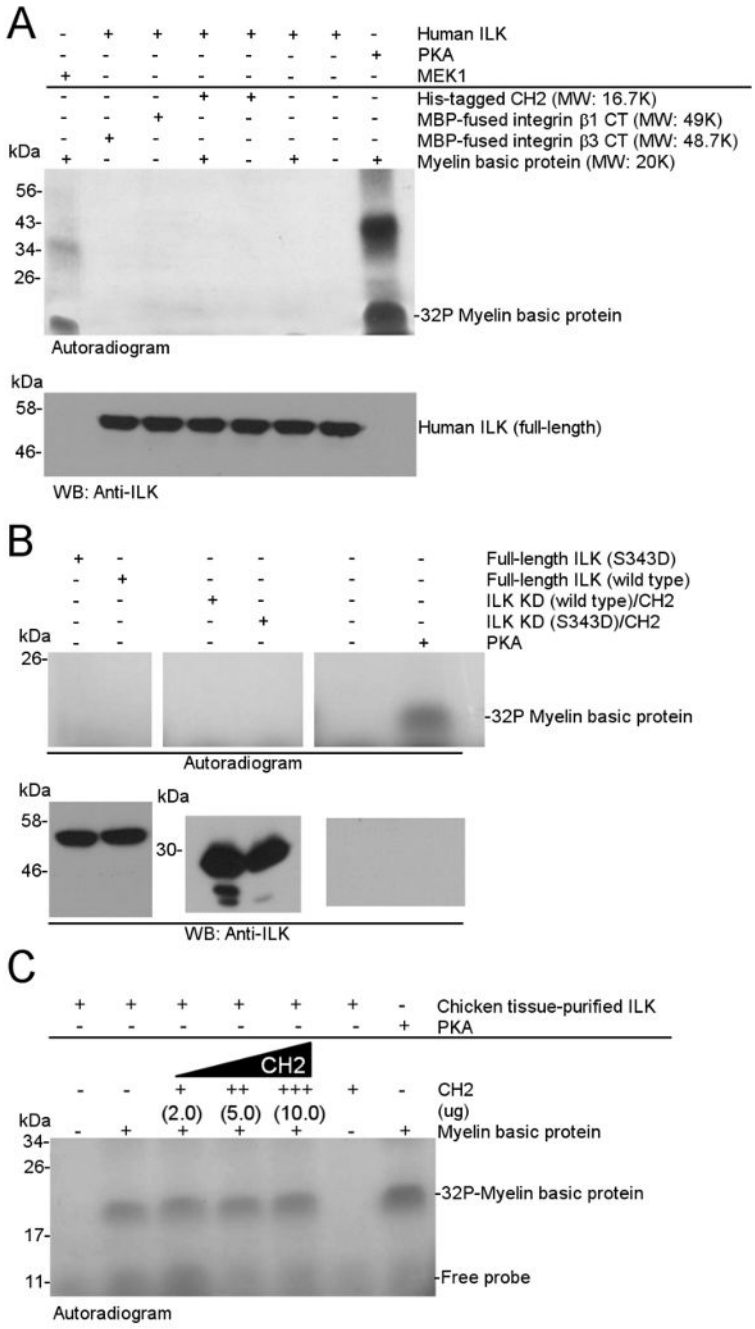

Figure 3. Biochemical Analysis of the ILK Kinase Activity

(**A**) Representative *in vitro* radioactive kinase assay data using bacterially purified recombinant full-length human ILK. The protein substrates are myelin basic protein (MW: 20K), myelin basic protein + CH2, CH2 alone, maltose binding protein (MBP)-fused integrin β1 CT, and MBP-fused integrin β3 CT. None of these substrates were phosphorylated as compared to the positive controls using bacterially purified PKA (SignalChem) and MEK (Millipore). The kinase reaction was also performed by adding 50 μM PIP3 (Echelon) or full-length α-parvin, but no effect was observed (data not shown). Mg concentration was also varied but no difference was observed (data not shown). (**B**) Effect of the S343D mutation on ILK activity. The S343D mutant of either full-length ILK or ILK KD did not show any phosphorylation on

NIH-PA Author Manuscript

NIH-PA Author Manuscript

NIH-PA Author Manuscript

myelin basic protein. Addition of 50 μM PIP3 into these kinase reactions also had no effect (not shown). Several other ILK mutants, A319D that mimics D166 in PKA, A319D/S343D, triple mutant A319D/N321K/S343D (N321K mimics K168 in PKA), were also examined to see if they may restore the kinase activity. However, none of them phosphorylated MBP (data not shown). Since ILK has multiple degraded catalytic features including distorted ATP/Mg binding, degenerate catalytic loop, and an unusual activation loop, simply converting some catalytic residues are apparently insufficient to recover the kinase activity. A similar case was found in STRADα pseudokinase, where converting key residues did not restore the kinase activity of the protein (Zeqiraj et al., 2009). (**C**) Kinase activity of partially purified ILK from chicken-tissue in the absence and presence of CH2. The exogenous substrate myelin basic protein was phosphorylated by the partially purified chicken kinase extract containing ILK. However, the phosphorylation was neither enhanced nor inhibited by addition of recombinant CH2. CH2 was not phosphorylated by ILK (lane 6 from left). The MBP-fused integrin β1 or β3 CTs were not phosphorylated either (data not shown). See also Figure S3.

NIH-PA Author Manuscript
NIH-PA Author Manuscript
NIH-PA Author Manuscript

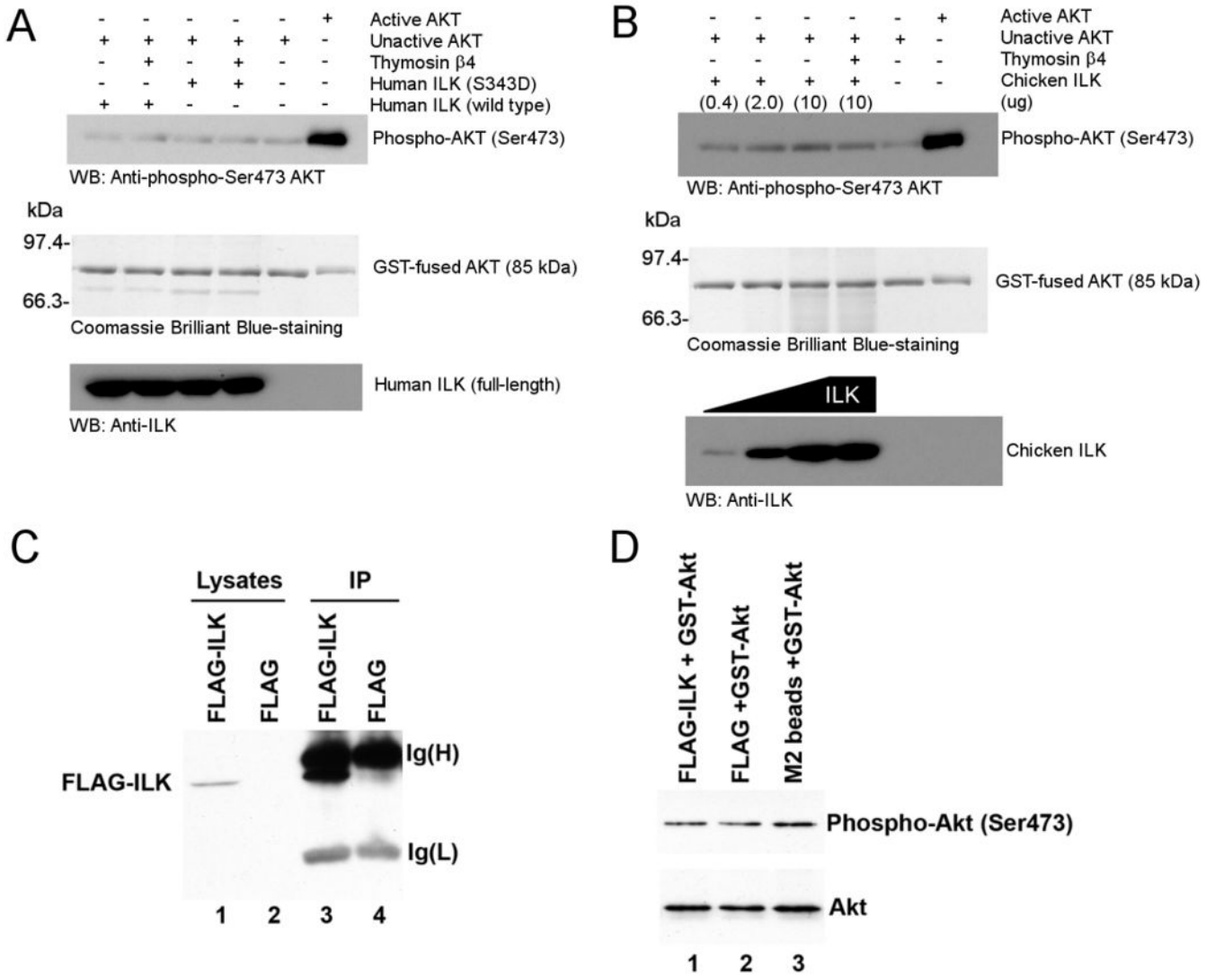

Figure 4. Effect of ILK on Akt Serine 473 Phosphorylation

(**A**) Effect of bacterially expressed full-length human ILK on Akt phosphorylation (S473). Note that the inactive GST-Akt (SignalChem) used as the substrate exhibits a basal phosphorylation on S473 (lane 5 from left) compared to the same amount of active Akt (lane 6 from left). Active Akt was prepared using the GST-fused active Akt (SignalChem) as a positive control (1 μg) in the same reaction buffer (50 μL in volume) without adding ILK and substrate. (**B**) Effect of chicken-tissue purified ILK on the Akt S473 phosphorylation. The amount of chicken ILK is shown in parentheses. (**C**) Overexpression of ILK in HEK 293 cells and the co-immunoprecipitation analysis. (D) Effect of the ILK immunoprecipitants on S473 phosphorylation of Akt. The fractions of FLAG-ILK (lane 1) and control FLAG (lane 2) immunoprecipitates, or anti-FLAG M2-conjugated beads (lane 3) were incubated with 1 μg of GST-Akt and analyzed by Western blotting with anti-phospho Akt S473 specific antibody. Note that the GST-fused Akt exhibits a basal phosphorylation on S473 (lane 3). No further phosphorylation of Akt on S473 was observed during the kinase reaction by the ILK immunoprecipitant (lane 1) as compared to the control by the FLAG only immunoprecipitant (lane 2). See also Figure S4.

NIH-PA Author Manuscript
NIH-PA Author Manuscript
NIH-PA Author Manuscript

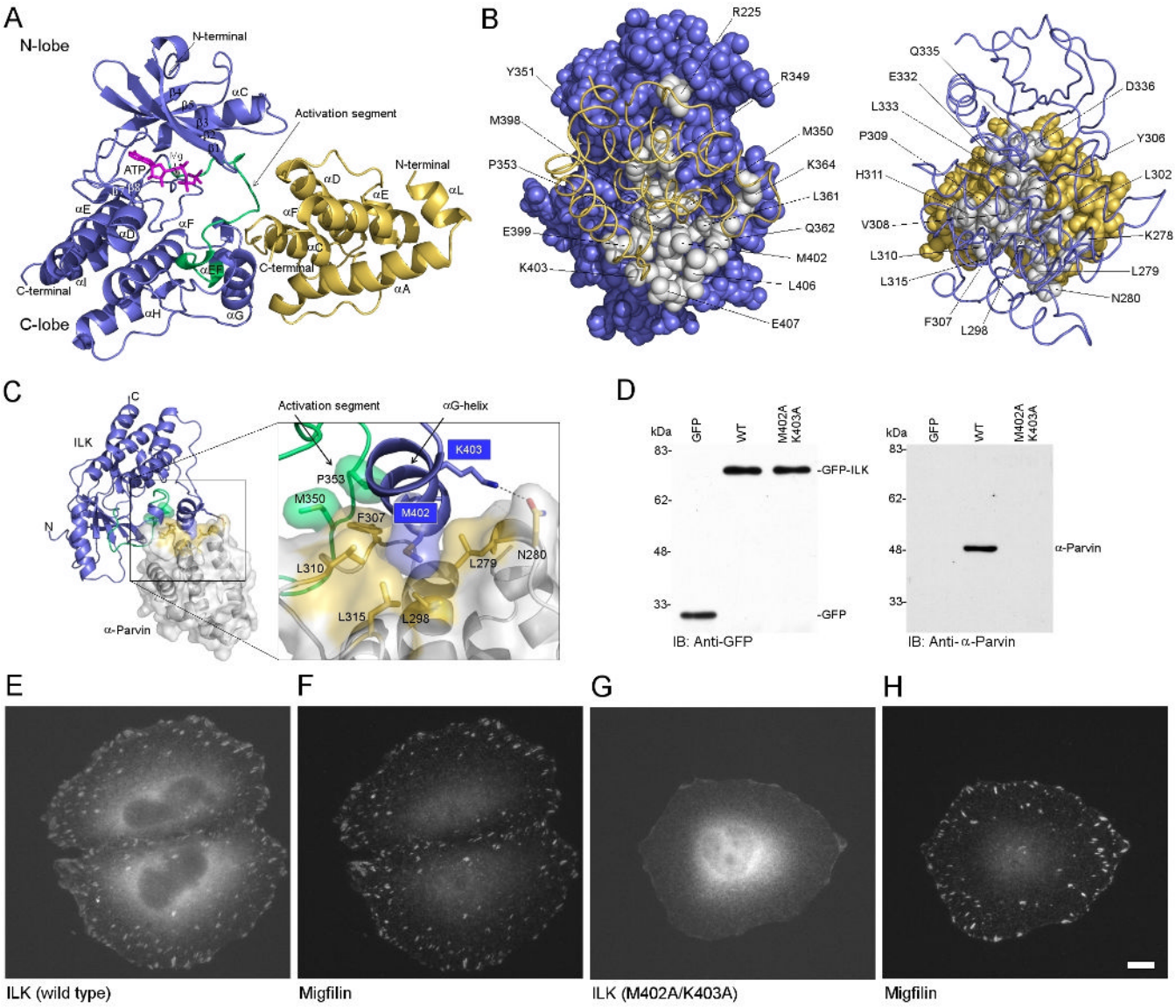

Figure 5. Determinants of the Pseudosubstrate Recognition by ILK

(**A**) Overall architecture of the ILK KD (blue) bound to CH2 (yellow). The activation segment is colored in green. The ATP molecule and magnesium ion are depicted in stick (magenta) and sphere (white) models, respectively. (**B**) Open-book view of the binding interface of the ILK KD-CH2 complex. Left panel: CH2-binding surface (gray) on ILK KD. The bound CH2 is shown in loop model (yellow) and ILK KD in surface model (blue). Right: ILK-binding surface (gray) on CH2. The bound ILK KD is shown in loop model (blue) and CH2 in surface model (yellow). All residues in the interface are labeled. (**C**) Involvement of the ILK αG-helix and activation loop in binding to CH2. Left: Ribbon model of the ILK KD/CH2 complex. The CH2 is depicted by the transparent surface model. Right: Close-up view of the hydrophobic and polar interactions between the G-helix in the ILK KD and α-parvin CH2. The ILK KD-binding hydrophobic patch on the CH2 is depicted in stick models and colored in yellow on the transparent surface model of CH2. M350 and P353 in the C-terminal activation segment that interact with CH2 are depicted in green stick and transparent models. (**D**) Identification of the critical residues involved in the ILK-CH2 interface. Left: Normal expression of GFP-tagged wild type and the mutant forms of ILK. GFP tagged wild type and M402A/K403A mutant

NIH-PA Author Manuscript

NIH-PA Author Manuscript

NIH-PA Author Manuscript

forms of ILK were immunoprecipitated from HeLa cells expressing the corresponding ILK proteins with an anti-GFP antibody. Right: Evaluation of the α-parvin binding. The immunoprecipitates were analyzed by Western blotting with anti-α-parvin antibody. (**E-H**) Focal adhesion localization of wild type and M402A/K403A mutant forms of ILK. HeLa cells expressing GFP-tagged wild type (**E** and **F**) and M402A/K403A mutant (**G** and **H**) forms of ILK were plated on fibronectin coated cover slips. The cells were stained with a mouse monoclonal antibody recognizing migfilin (as a marker of FAs) and Rhodamine Red^{TX}-conjugated anti-mouse IgG antibodies. The GFP-tagged wild type (**E**) and mutant (**G**) forms of ILK and migfilin (**F** and **H**) were observed under a fluorescence microscope. Bar indicates 10 μm. See also Figure S5.

NIH-PA Author Manuscript
NIH-PA Author Manuscript
NIH-PA Author Manuscript

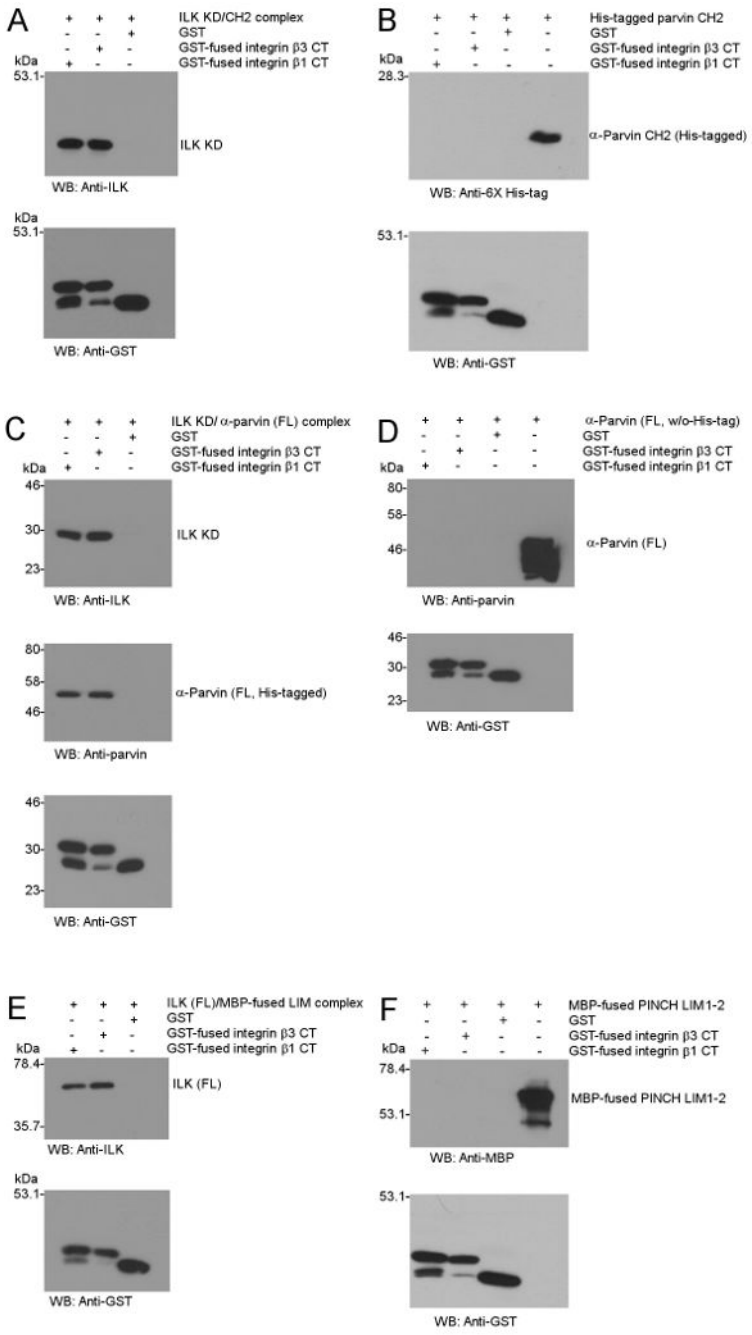

Figure 6. Integrin-Binding to ILK

(**A**) Binding of the ILK KD-CH2 complex to GST-integrin β1 CT or β3 CT using pull-down assays. Western blots are shown for the bound ILK KD with anti-ILK monoclonal antibody or the GST-integrin CTs and control GST with anti-GST monoclonal antibody. (**B**) Control experiment of no direct binding of CH2 to integrin CTs. (**C**) Binding of the ILK KD-α-parvin (full-length) complex to the integrin CTs. Parvin was detected using anti-parvin antibody raised against the parvin N-terminal region, showing that it is associated with the ILK/integrin interaction by binding to ILK. (**D**) Control experiment of no direct parvin-binding to integrins. (**E**) Binding of full-length ILK to GST-integrin β1 CT or β3 CT. The Western blotting analysis is shown for the bound full-length ILK with anti-ILK monoclonal antibody. (**F**) Control

NIH-PA Author Manuscript

NIH-PA Author Manuscript

NIH-PA Author Manuscript

experiment showing no direct binding of MBP-fused PINCH LIM1-2 to the integrin CTs. All the binding experiments were repeated three times. See also Figure S6.

NIH-PA Author Manuscript
NIH-PA Author Manuscript
NIH-PA Author Manuscript

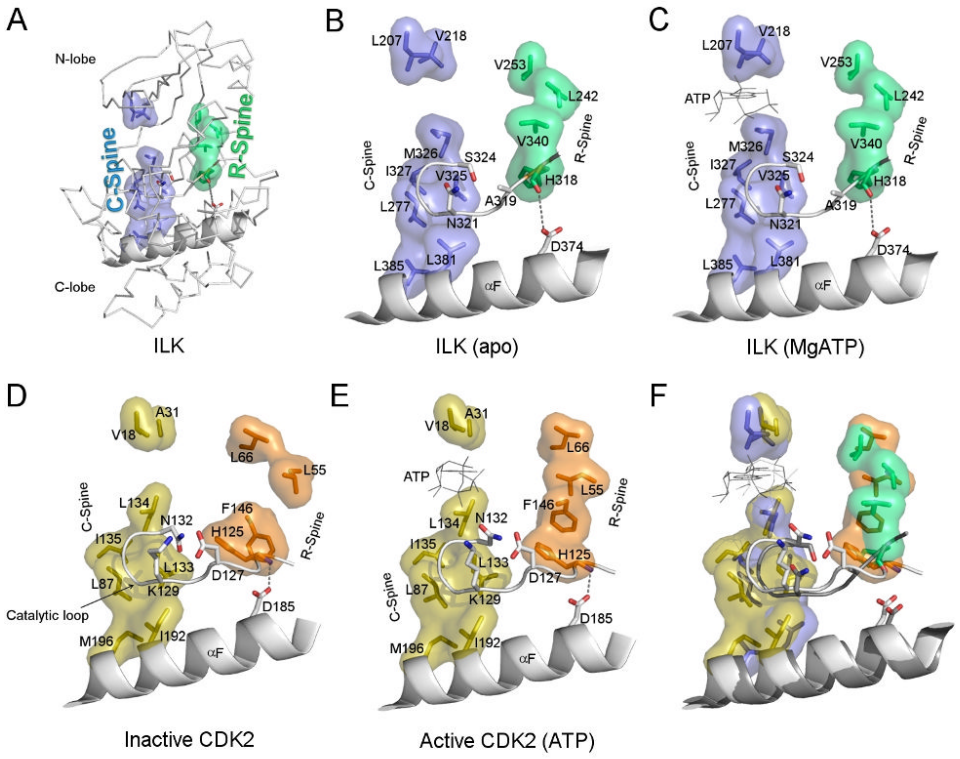

Figure 7. Hydrophobic spine motifs in active kinases and ILK

(**A**) Overall structure of the ILK KD and location of the hydrophobic spine motifs. The hydrophobic residues in the regulatory (R) and catalytic (C) spines are depicted in stick models rendered in the transparent surfaces colored in green and blue, respectively. The conserved αF-helix and the aspartate residue D374 are highlighted. (**B**) Close-up view of the R- and C-spine motifs in the ILK KD apo form. (**C**) Close-up view of the R- and C-spine motifs in the ILK KD bound to Mg and ATP. ATP has no effect on the spines. (**D**) Close-up view of the R- and C-spine motifs in inactive protein kinase CDK2 (PDB entry 1HCL) (apo form). (**E**) Close-up view of the R- and C-spine motifs in the active CDK2 (PDB entry 1FIN) bound to ATP. Note that the R-spine motif is disrupted in (**D**), as compared to those in ILK KD in (**C**) and active CDK2 in (**E**). (**F**) Overlay of the R-, C-spine motifs, and other key segments between the ATP-bound ILK KD and the active CDK2, showing a similar spine formation between ILK and active CDK2 kinase. See also Figure S7.

NIH-PA Author Manuscript

NIH-PA Author Manuscript

NIH-PA Author Manuscript

Table 1
Data collection and refinement statistics

Data collection			
Data sets	SeMet (apo)		Mg-ATP
Space group	$P2_1$	$P2_1$	$P2_1$
Cell dimensions (Å, °)			
a	44.38	44.50	44.13
b	117.72	118.07	117.10
c	47.34	47.44	47.39
β	101.68	101.66	101.96
	Peak	Inflection	
Wavelength (Å)	0.97880	0.97900	1.5418
Resolution range (Å)	50 – 1.75	50 – 1.8	46.33 – 2.00
Highest resolution shell (Å)	1.78 – 1.75	1.83 – 1.80	2.07 – 2.00
No. observations	360348	334806	172449
No. unique reflections	94370	87704	31165
$I/\sigma I$	28.2 (2.3)	27.1 (1.9)	12.2 (7.8)
Completeness (%)	99.9 (96.9)	99.9 (100.0)	98.3 (98.8)
R_{sym}	0.058 (0.440)	0.070 (0.813)	0.098 (0.136)
Redundancy	3.80 (3.40)	3.80 (3.70)	5.53 (6.09)
Phasing			
No. of sites	16		
Figure of merit[1]	0.51/0.71		
Refinement			
Resolution limit (Å)	1.8		2.00
No. unique reflections	41751		31052
R_{work}	0.200		0.199
R_{free}	0.236		0.203
No. non-hydrogen atoms			
Protein	3148		3157
Ligand/ion	0		31/1
Water	298		309
B-factors (Å^2)			
Protein (overall)	31.8		26.6
ILK	21.7		18.8
CH2	41.8		34.4
Ligand/ion	N/A		16.6/19.0
Water	35.3		31.6
r.m.s. deviations			
Bond lengths (Å)	0.016		0.020

NIH-PA Author Manuscript

NIH-PA Author Manuscript

NIH-PA Author Manuscript

Bond angles (°)	1.4		1.6

Highest resolution shell is shown in parenthesis.

[1] Prior to/post density modification.